MEC-2 and MEC-6 in the *Caenorhabditis elegans* Sensory Mechanotransduction Complex: Auxiliary Subunits that Enable Channel Activity

Austin L. Brown,[1] Zhiwen Liao,[2] and Miriam B. Goodman[1,2]

[1]Biophysics Program and [2]Department of Molecular and Cellular Physiology, Stanford University, Stanford, CA 94305

The ion channel formed by the homologous proteins MEC-4 and MEC-10 forms the core of a sensory mechanotransduction channel in *Caenorhabditis elegans*. Although the products of other *mec* genes are key players in the biophysics of transduction, the mechanism by which they contribute to the properties of the channel is unknown. Here, we investigate the role of two auxiliary channel subunits, MEC-2 (stomatin-like) and MEC-6 (paraoxonase-like), by coexpressing them with constitutively active MEC-4/MEC-10 heteromeric channels in *Xenopus* oocytes. This work extends prior work demonstrating that MEC-2 and MEC-6 synergistically increase macroscopic current. We use single-channel recordings and biochemistry to show that these auxiliary subunits alter function by increasing the number of channels in an active state rather than by dramatically affecting either single-channel properties or surface expression. We also use two-electrode voltage clamp and outside-out macropatch recording to examine the effects of divalent cations and proteases, known regulators of channel family members. Finally, we examine the role of cholesterol binding in the mechanism of MEC-2 action by measuring whole-cell and single-channel currents in MEC-2 mutants deficient in cholesterol binding. We suggest that MEC-2 and MEC-6 play essential roles in modulating both the local membrane environment of MEC-4/MEC-10 channels and the availability of such channels to be gated by force in vivo.

INTRODUCTION

Sensing force is ubiquitous in cellular life, with uses ranging from protection from osmotic shock in bacteria (Levina et al., 1999) to the appreciation of the softest touch on human skin (Johansson and Vallbo, 1979). Among medically relevant modes of force transduction in humans are flow regulation in the kidney, blood pressure regulation in vasculature, hearing, proprioception in musculature, nociception, and cutaneous touch. Each of these processes is likely to involve many molecules that have proven difficult to identify, possibly due to their rarity. In contrast, genetic analysis of touch in *Caenorhabditis elegans* has proven fruitful for identifying the molecular components of mechanotransduction machinery, including four membrane proteins (MEC-2, MEC-4, MEC-6, and MEC-10). These proteins form amiloride-sensitive, Na^+-selective sensory mechanotransduction channels in the touch receptor neurons (TRNs) responsible for detecting low-intensity touches in *C. elegans* (O'Hagan et al., 2005). In *Xenopus* oocytes, these proteins also form amiloride-sensitive Na^+ channels (Chelur et al., 2002; Goodman et al., 2002a).

MEC-4 and MEC-10 are pore-forming subunits that belong to the superfamily of degenerin/epithelial sodium channel (DEG/ENaC) ion channel proteins that are conserved in metazoans. DEG/ENaC proteins are predicted to share a common topology consisting of two transmembrane helices, intracellular N and C termini, and a large extracellular domain (Kellenberger and Schild, 2002). Recent structural data confirm this topology (Jasti et al., 2007). MEC-2 and MEC-6 are auxiliary subunits required for channel function in vivo (O'Hagan et al., 2005). Replacing the wild-type alanine at the degenerin (*d*) position in MEC-4 (A713) or MEC-10 (A673) with residues larger than cysteine induces TRN degeneration in vivo (Driscoll and Chalfie, 1991; Huang and Chalfie, 1994) and increases channel open probability in *Xenopus* oocytes (Brown et al., 2007). The *d* position is at the extracellular end of the second transmembrane domain and its side chain interacts with the first transmembrane domain of the adjacent subunit (Jasti et al., 2007). This structural observation is consistent with our finding that mutations at the *d* position in MEC-10 can both enhance and suppress gain-of-function mutations in MEC-4 (Brown et al., 2007). Taking advantage of the increased open probability in mutants, we study gain-of-function mutants of both MEC-4 and MEC-10 with an alanine to threonine substitution at the *d* position. For clarity, we refer to these mutants as MEC-4d and MEC-10d and to heteromeric channels as MEC-4d/10d channels.

Correspondence to Miriam B. Goodman: mbgoodman@stanford.edu

The online version of this article contains supplemental material.

Abbreviations used in this paper: DEG, degenerin; ENaC, epithelial sodium channel; HDL, high-density lipoprotein; PHB, prohibitin homology; PON, paraoxonase; TRN, touch receptor neuron.

The Rockefeller University Press $30.00
J. Gen. Physiol. Vol. 131 No. 6 605–616
www.jgp.org/cgi/doi/10.1085/jgp.200709910

Defects in the genes encoding MEC-2 and MEC-6, which are coexpressed with MEC-4 and MEC-10 in TRNs (Lai et al., 1996; Chelur et al., 2002; Goodman et al., 2002a), suppress degeneration (Chalfie and Wolinsky, 1990; Huang and Chalfie, 1994), suggesting that these proteins might be critical for channel function. Consistent with this idea, MEC-2 and MEC-6 dramatically enhance macroscopic currents carried by heteromeric MEC-4d/10d channels in *Xenopus* oocytes without increasing the expression of either protein in the plasma membrane. Together, MEC-2 and MEC-6 increase macroscopic current by more than 100-fold (Chelur et al., 2002; Goodman et al., 2002a). It is not known how these auxiliary proteins achieve their remarkable effect without increasing surface expression. All available evidence suggests that the effects of MEC-2 and MEC-6 on current are similar in wild-type and degenerin mutant channels (Chelur et al., 2002; Goodman et al., 2002a). Under this assumption, we use mutant channels with increased open probability to facilitate measurement of the effects of auxiliary subunit coexpression.

Like some other prohibitin-homology (PHB) domain proteins (SMART database; http://smart.embl-heidelberg.de), MEC-2 is associated with the inner leaflet of the plasma membrane and does not cross the bilayer (Huang et al., 1995). In its central PHB domain, MEC-2 is 65% identical to human stomatin and 62% identical to SLP-3. In mice, both stomatin and SLP-3 are expressed in the cell bodies and nerve terminals of dorsal root ganglion sensory neurons (Mannsfeldt et al., 1999; Wetzel et al., 2007). Loss of stomatin reduces the response of a single class of somatosensory neurons to mechanical stimuli (Martinez-Salgado et al., 2007). SLP-3 is required in several classes and also plays a critical role in texture discrimination (Wetzel et al., 2007). MEC-2 binds the N-terminal domain of MEC-4 through its central PHB domain (Zhang et al., 2004a). MEC-2 is palmitoylated and binds cholesterol directly (Huber et al., 2006). The double-cysteine mutant MEC-2 (C140/174A) is no longer palmitoylated and has reduced cholesterol-binding activity (Huber et al., 2006). MEC-2(P134S), which recapitulates the *u274* allele of the *mec-2* gene, fails to bind cholesterol in vitro, but localizes to the plasma membrane in HEK293T cells and binds to DEG/ENaC proteins (Huber et al., 2006). Considered together with the finding that *mec-2(u274)* animals are touch insensitive, these data suggest that cholesterol binding is required for normal MEC-2 activity. Both palmitoylation and cholesterol binding are likely to fine tune the association between MEC-2, the pore-forming subunits MEC-4 and MEC-10, and the plasma membrane and may recruit specialized lipid microdomains to the vicinity of the MEC-4 channel. MEC-2 is not the only PHB protein likely involved in *C. elegans* touch sensation. UNC-24 is coexpressed with MEC-2 in the TRNs (Zhang et al., 2004a,b) and several PHB proteins, including UNC-24, appear to associate with cholesterol-rich, detergent-resistant membrane fractions (Sedensky et al., 2004).

With a short cytoplasmic N terminus and a single transmembrane domain, the majority of the MEC-6 protein is extracellular (Chelur et al., 2002). In its extracellular domain, MEC-6 is homologous to human paraoxonase (PON1), an enzyme that hydrolyzes organophosphates and has a role in preventing heart disease through its association with high-density lipoprotein (HDL) particles (Draganov et al., 2000). By structural and functional criteria, several residues in PON1 are believed to be important for enzymatic activity (Harel et al., 2004; Yeung et al., 2005). Only one of these residues is conserved in MEC-6, N143, suggesting that MEC-6 lacks enzymatic activity. Association between PON1 and HDL particles is believed to involve two amphipathic helices, one of which is proposed to extend hydrophobic aromatic residues into the lipid interface (Harel et al., 2004). This domain, including a series of aromatic residues arranged along one side of the helix, is conserved in MEC-6 (unpublished data) and may facilitate association between MEC-6 and the outer leaflet of the plasma membrane. Wild-type MEC-6 is required for proper localization of the channel complex in vivo but not in oocytes (Chelur et al., 2002). Thus, MEC-6 has at least two roles, only one of which is recapitulated in heterologous cells.

Among known regulators of ENaC activity are various serine proteases. There is a growing body of evidence that proteases can modify ENaC activity in diverse ways (for review see Planes and Caughey, 2007). For example, furin seems to be involved in post-translational processing in the endoplasmic reticulum (Hughey et al., 2004), membrane-bound channel-activating proteases (CAPs) regulate the channel after insertion into the membrane (Vallet et al., 2002), and soluble proteases such as trypsin activate channels dwelling in a near-silent state (Caldwell et al., 2004), though it has been suggested that this activation may be indirect (Bengrine et al., 2007).

Here, we use mutations at the *d* position to render channels constitutively active in *Xenopus* oocytes and use single-channel, macropatch, and whole-cell recording to investigate the mechanism by which the auxiliary subunits MEC-2 and MEC-6 enhance channel activity. We explore the roles of MEC-2 and MEC-6 in block by divalent ions, sensitivity to proteases, single-channel properties, and surface expression. Finally, we demonstrate that MEC-2 and MEC-6 have a role in promoting an active state of the channel and show that this activity is lost in MEC-2 mutants deficient in cholesterol binding.

MATERIALS AND METHODS

Molecular Biology

Constructs encoding full-length MEC-4d and MEC-10d as well as myc-tagged MEC-4d were propagated in SMC4 bacteria (American

Type Culture Collection accession no. PTA-4084) as previously described (Goodman et al., 2002a; Brown et al., 2007). Constructs encoding full-length, wild-type MEC-2 and MEC-6 were propagated in XL1-Blue. MEC-2 mutants were obtained by in vitro mutagenesis (Quik-Change Kit, Invitrogen).

Heterologous Expression

Capped cRNAs were synthesized in vitro (mMESSAGE mMACHINE T7 kit, Ambion) and quantified spectroscopically. *Xenopus laevis* oocytes were isolated and injected with 50 nl of cRNA solution. Except where indicated, we injected equal amounts of MEC-4d, MEC-10d, and MEC-2 cRNA and one tenth that amount of MEC-6 cRNA. (Larger amounts of MEC-6 cRNA induce a nonspecific, amiloride-insensitive current that complicates analysis [Chelur et al., 2002].) Oocytes were maintained at 18°C in modified L-15 medium supplemented with gentamicin (144 µM) and amiloride (300 µM) until recording.

Injection conditions were modified according to the experimental goal. For whole-cell recordings or macropatches with many active channels, 2.5–5 ng of MEC-4d cRNA was injected. For single channel recordings, both the amount of cRNA injected and days of incubation were optimized to maximize the chance of obtaining single-channel patches. With MEC-2 and MEC-6 present, less cRNA and shorter incubations were required to obtain a similar channel density. For single-channel recordings, conditions were (a) for MEC-4d/10d alone, 5–10 ng each, 4–10 d; (b) for MEC-4d/10d + MEC-2, 2–5 ng each, 2–4 d; (c) for MEC-4d/10d + MEC-6, 1–2 ng each, 3–6 d; (d) for MEC-4d/10d + MEC-2 + MEC-6, 0.25–1 ng each, 1–2 d.

Electrophysiology: Whole-Cell Recording

Membrane current was measured by two-electrode voltage-clamp (OC-725C, Warner Instruments, LLC) at room temperature (21–24°C). Electrodes (1–4 MΩ) were fabricated on a horizontal puller (P-97; Sutter Instruments) and filled with 3 M KCl. Analogue signals were filtered at 200 Hz (8-pole Bessel filter) and sampled at 1 kHz. A 60-Hz notch filter was used to minimize line noise. Oocytes were superfused with control saline containing (in mM) Na-gluconate (100), KCl (2), $MgCl_2$ (2), $CaCl_2$ (1), and Na-HEPES (10), adjusted to pH 7.4 with NaOH. The amplitude of amiloride-sensitive current was measured as the difference between current measured at −85 mV in the absence and presence of 300 µM amiloride. For protease experiments, 200 µg/ml chymotrypsin was added to control saline.

Electrophysiology: Outside-Out Patches

Vitelline membranes were removed from oocytes manually following incubation in a hypertonic solution composed of (in mM) NMDG-aspartate (220), $MgCl_2$ (1), EGTA (10), KCl (2), HEPES (10), and amiloride (0.3), adjusted to pH 7.4 with NMDG. Pipettes (2–8 MΩ) were pressure polished (Goodman and Lockery, 2000) and filled with a calcium-buffered saline solution containing (in mM) Na-gluconate (100), NaCl (2), $CaCl_2$ (2), Na_2EGTA (5), and HEPES (10), adjusted to pH 7.4 with NaOH. External solutions were identical to pipette solution, except where Ca^{2+} (1–10 mM), Mg^{2+} (1–10 mM), or amiloride (50 µM) were added. Where divalent ions were added, Na_2EGTA was omitted from external solutions. Single-channel and macropatch currents were recorded in an outside-out configuration with a patch-clamp amplifier (WPC-100 E.S.F.; Bioscience Tools), filtered (F_c = 1–5 kHz, 4-pole Bessel filter), and digitized at a rate that was at least three times the filtering frequency. Pulse/Pulsefit or Patchmaster software (HEKA Electronics Inc.) was used to control data acquisition; Igor Pro (Wavemetrics) and QuB Software (The Research Foundation of the State University of New York; http://www.qub.buffalo.edu) were used for single-channel data analysis. Single-channel conductance and open probability were calculated from all-points histograms derived from leak-subtracted records that were 4.7 min long on average. We corrected for nonspecific leak currents by fitting a line to time intervals in which all channels were closed and subtracting the result from the data.

MEC-4 Surface Expression

Analysis of surface protein closely followed methods described previously (Chillaron et al., 1997; Goodman et al., 2002a). Between 100 and 150 intact oocytes were selected 4 d after cRNA injection, placed in a Petri dish coated with agarose (1% wt/vol in OR-2) and washed three times in OR-2 medium (82.5 mM NaCl, 2.5 mM KCl, 1 mM $MgCl_2$, 5 mM HEPES adjusted to pH 7.6 with NaOH). Surface proteins were labeled by incubating oocytes in OR-2 medium containing membrane-impermeant reagent EZ-Link Sulfo-NHS-LC-Biotin (Pierce Chemical Co., 16 mg/ml) for 10 min. The reaction was stopped by adding 2 ml of 500 mM glycine, pH 7.5 (1 min), and washed in 500 mM glycine (three times) and fresh OR-2 (three times). Equal numbers of intact oocytes from each experimental condition were selected and transferred to microcentrifuge tubes and homogenized by gentle trituration in lysis buffer, LyB (10 µl per oocyte; 2% Nonidet P-40, 150 mM NaCl, 2 mM $CaCl_2$, 20 mM Tris-HCl, pH 7.4, plus 1 protease inhibitor cocktail tablet [Roche Applied Science] into 10 ml of lysis buffer before use). The homogenate was centrifuged twice (1,000 *g*, 10 min, 4°C) to remove the yolk platelets. The supernatant was sonicated (2 min), centrifuged (1,000 *g*, 10 min, 4°C), and dialyzed overnight at 4°C against streptavidin buffer (SAv buffer: 0.3% Nonidet P-40, 500 mM NaCl, 1 mM $CaCl_2$, 1 mM $MgCl_2$, 10 mM Tris-HCl, pH 8) in Slide-A-Lyzer Dialysis Cassettes (3.5K MWCO, Pierce Chemical Co.). The homogenate was centrifuged (1,000 *g*, 10 min, 4°C) and biotinylated proteins were isolated using streptavidin-agarose beads (Thermo Scientific). Beads were recovered by centrifugation (833 *g*), washed in SAv buffer (three times). Protein was eluted by boiling beads in Laemmeli buffer and 2-mercaptoethanol for 2 min. Proteins were separated by SDS-PAGE (100–130 oocyte equivalents per lane). Myc-tagged MEC-4d was detected in Western blots using an HRP-conjugated c-Myc antibody (9E10, Santa Cruz Biotechnology, 1:500 dilution in PBS-T [137 mM NaCl, 2.7 mM KCl, 10 mM Na_2HPO_4, 1.8 mM KH_2PO_4, 0.1% Tween-20] with 5% nonfat dry milk). HRP was detected using chemiluminescence (ECL plus, GE Life Sciences) and blots were visualized with a CCD-based luminometer (Fluorchem 8800 with Multiimage light chamber chemiluminescent filter, Alpha Innotech). Digital images were used to determine the relative amounts of protein by densitometry in ImageJ (NIH).

MEC-2 Expression

10 intact oocytes were selected 4 d after cRNA injection and homogenized by gentle trituration in LyB with protease inhibitor (see above). The homogenate was centrifuged (1,000 *g*, 10 min, 4°C) and separated by SDS-PAGE (two oocyte equivalents per lane). MEC-2 was detected by Western blotting with anti-MEC-2 rabbit primary (Zhang et al., 2004a) and HRP-conjugated secondary (Santa Cruz Biotechnology), blocked, washed and visualized with the same reagents as for MEC-4 Western blots (above).

Cholesterol Depletion

Immediately after injection, oocytes were divided into two groups. The control group was incubated in L-15 supplemented with gentamicin (144 µM) and amiloride (300 µM). The experimental group was also treated with methyl-β-cyclodextrin (5 mM) and pravastatin (250 µM). Amiloride-sensitive currents were measured 4–6 d later. Between 5 and 17 oocytes in each group were tested.

Reagents

Except as noted above, chemicals were obtained from Sigma-Aldrich. Amiloride was diluted from 0.1 M stock solutions in DMSO.

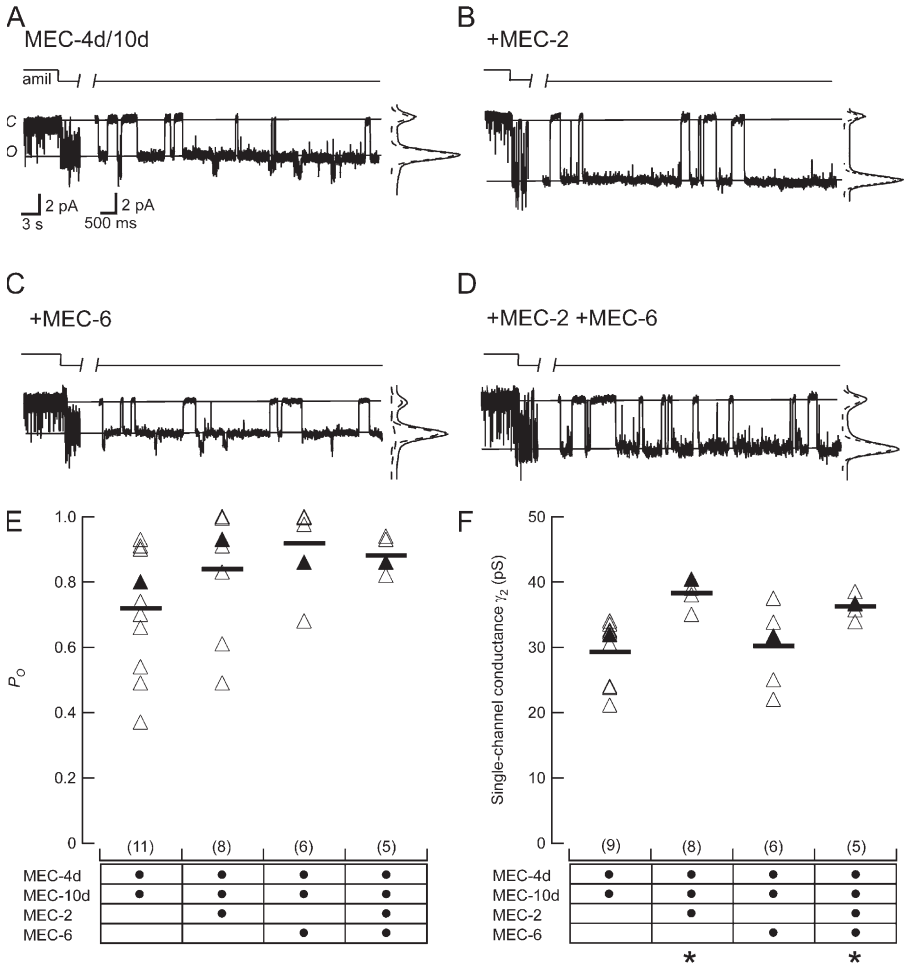

Figure 1. Single-channel recordings from outside-out patches. (A) MEC-4d/10d only. (B) MEC-4d/10d + MEC-2. (C) MEC-4d/10d + MEC-6. (D) MEC-4d/10d + MEC-2 + MEC-6. In A–D, two sections are shown: the left demonstrates the sensitivity of the channel to amiloride (50 μM), while the right shows the channel behavior in control saline. $V_{hold} = -150$ mV. Closed and open states are labeled *C* and *O* respectively and indicated by solid lines. To the right of each record is an all-points histogram of the same trace; dotted lines represent Gaussian fits to each peak. Open probability (E) and single-channel conductance (F) of patches containing a single channel. Data are summarized in Table I. Closed triangles represent the example patches shown in A–D. Bars indicate mean values for each isoform. Number of patches indicated in parentheses. *, significantly different from MEC-4d/10d ($P < 0.01$).

Statistics and Curve Fitting

Curve fitting was performed with nonlinear least-squares regression in Igor Pro (Wavemetrics). Statistical comparisons were performed as Student's *t* test assuming unequal variances and analysis of variance (ANOVA). ANOVA results are expressed as $F(a,b) = c$, $P = d$ where a and b are the degrees of freedom between and within groups, c is the F value, and d is the probability in insignificance.

Dwell-Time Analysis

Open and closed channel dwell times were generated from single-channel idealizations determined using QuB. All single-channel patches were used to generate average dwell times, τ_{open} and τ_{closed}; only patches with more than 1,000 events were used to generate histograms of dwell times. Dwell times were converted into histograms with logarithmic bins and plotted with a square-root ordinate and fit with a sum of exponentials, as previously described (Sigworth and Sine, 1987). At small dwell times, some bins contain no even multiple of the sampling interval and are empty as an artifact of logarithmic binning. To lessen this effect for display purposes, histograms were smoothed across adjacent bins.

Online Supplemental Material

The online supplemental material (Figs. S1 and S2) is available at http://www.jgp.org/cgi/content/full/jgp.200709910/DC1). Fig. S1 compares dose–response curves for blockade by amiloride in the presence and absence of divalent cations. Fig. S2 shows the surface expression of myc-tagged MEC-4d channels in the presence and absence of MEC-2 and MEC-6.

RESULTS

To measure the effects of MEC-2 and MEC-6 on open probability (P_o), single channel conductance (γ), and open- and closed-state dwell times, we excised outside-out patches from *Xenopus* oocytes injected with the cRNA encoding MEC-4d/10d alone, with MEC-2, with MEC-6, and with both MEC-2 and MEC-6. In all cases, we observe channels that are constitutively active and blocked by micromolar concentrations of amiloride. Channels with these characteristics are never observed when MEC-4d is omitted ($n = 18$ patches, unpublished data) or in control cells injected with water ($n = 14$ patches, unpublished data). This is consistent with results in vivo (O'Hagan et al., 2005) and in whole-cell voltage clamp (Goodman et al., 2002a) and demonstrates that MEC-4 is necessary for channel formation. It is also sufficient: oocytes expressing only MEC-4d express both macroscopic amiloride-sensitive currents (Goodman et al., 2002b) and single amiloride-sensitive channels ($n = 1$, unpublished data).

Neither MEC-2 nor MEC-6 Affects Average P_o nor Dwell Times in the Open or Closed State

Single channels of the four heteromeric channel complexes studied in this report exhibited similar characteristics

TABLE I

Single-Channel Properties of MEC-4d/10d Channels and Effects of Auxiliary Subunits

	γ_1 (pS)	P_{o1}	γ_2 (pS)	P_{o2}	$\langle\gamma\rangle$ (pS)	P_o
MEC-4d/10d	19.3 ± 4.3 (11)	0.38 ± 0.27 (11)	29.3 ± 4.9 (11)	0.42 ± 0.33 (11)	17.0 ± 6.8 (11)	0.72 ± 0.20 (11)
+MEC-2	ND	ND	38.3 ± 1.6 (8)[a]	NA	31.8 ± 7.2 (8)[a]	0.79 ± 0.26 (8)
+MEC-6	ND	ND	30.2 ± 5.7 (6)	NA	24.9 ± 6.1 (6)[a]	0.72 ± 0.42 (6)
+MEC-2 +MEC-6	23.1 ± 2.5 (5)	0.46 ± 0.27 (5)	36.3 ± 1.6 (5)[a]	0.42 ± 0.29 (5)	25.6 ± 5.3 (5)[a]	0.89 ± 0.04 (5)

P_o ANOVA: $F(3,26) = 2.06$, P = 0.13. γ ANOVA: $F(3,24) = 9.3$, P < 0.0005.

[a]P < 0.01 by one-way *t* test compared to MEC-4d/10d.

to one another (Fig. 1), including subconductance states similar to those reported previously for homomeric MEC-4 channels (Brown et al., 2007). While we observed a range of P_o values for each channel complex, average values for P_o showed no significant dependence on the presence or absence of MEC-2, MEC-6, or both proteins (Fig. 1 E and Table I).

We also examined channel kinetics and performed dwell-time analyses. We did not observe any MEC-2– or MEC-6–dependent changes in the average open- or closed-state lifetimes (Tables II and III). Regardless of the channel isoform being studied, all single-channel dwell-time histograms demonstrated the existence of multiple closed and open states. Fig. 2 shows dwell-time histograms of open and closed times for a sample patch containing MEC-4d/10d + MEC-2 + MEC-6. Most (8/12) patches required three open and three closed states to generate satisfactory fits. The remaining four patches required either only two open or two closed states to generate an adequate fit. In each case, fit quality was examined by measuring sum-squared error (SSE) as a function of the number of states. Generally, SSE decreased significantly upon addition of a second and a third state, but was insensitive to the addition of a fourth, fifth, or sixth state (unpublished data). Similar to average lifetimes, dwell times of individual states extracted from fits to histograms do not demonstrate any significant dependence on the presence or absence of auxiliary subunits (Tables II and III).

MEC-2, but not MEC-6 Increases Single Channel Conductance

We did observe one significant effect on single channel properties; with MEC-2 present, the single-channel conductance of the larger subconductance state (γ_2) is increased by 30% ($P < 10^{-5}$) (Fig. 1 and Table I). While robust and reproducible, this difference in γ_2 would account for only ~1% of the observed ~40-fold increase in whole-cell current (Goodman et al., 2002a) and NP_O (see below) produced by MEC-2.

MEC-2 and MEC-6 Increase NP_O

Based on these findings, we predicted that MEC-2 and MEC-6 would enhance *NPo* in multichannel patches. Since *N* is the number of active channels in the patch (rather than the total number of proteins), such an effect is compatible with biochemical evidence showing that neither MEC-2 nor MEC-6 increase surface expression of MEC-4 or MEC-10 (see Chelur et al., 2002; Goodman et al., 2002a; and Fig. S2). Membrane patches from cells coinjected with 5–10 ng of cRNA encoding MEC-4d and MEC-10d rarely contained more than one channel. Thus, in the absence of MEC-2 and MEC-6, NP_o is <1. Consistent with our prediction, coinjecting MEC-2 increases NP_o to 33 ± 6 ($n = 6$), coinjecting MEC-6 gives $NP_O = 61 \pm 24$ ($n = 7$), and coinjecting both auxiliary subunits gives $NP_O = 718 \pm 202$ ($n = 10$). Thus, coinjecting MEC-2 and MEC-6 cRNA increases current to an even greater extent than predicted from whole-cell reports (200–400-fold) (Chelur et al., 2002; Goodman et al., 2002a).

Calcium Blocks and Permeates Heteromeric MEC-4d/10d Channels

In initial single-channel recordings, we observed only brief openings suggestive of fast, flickering blockade (unpublished data), which was reduced when divalent cations were removed from recording solutions. To test if this block was indeed due to Ca^{2+} and Mg^{2+} ions, we systematically varied the concentration of divalent

TABLE II

Closed-State Dwell Times of Single MEC-4d/10d Channels and Effects of Auxiliary Subunits

	$\langle\tau_c\rangle$(ms)	P_{c1}	τ_{c1} (ms)	P_{c2}	τ_{c2} (ms)	P_{c3}	τ_{c3} (ms)
MEC-4d/10d	81 ± 21 (11)	0.66 (3)	0.92 (3)	0.21 (3)	15 (3)	0.12 (1)	180 (1)
+MEC-2	54 ± 30 (7)	0.83 (3)	0.88 (3)	0.10 (2)	6.8 (2)	0.06 (2)	88 (2)
+MEC-6	37 ± 10 (4)	0.66 (2)	1.2 (2)	0.22 (2)	10 (2)	0.12 (2)	86 (2)
+MEC-2 +MEC-6	52 ± 36 (5)	0.69 (4)	1.8 (4)	0.13 (3)	6.6 (3)	0.18 (4)	147 (4)

Average closed-time, $\langle\tau_c\rangle$, ANOVA: $F(3,22) = 0.59$, P = 0.63

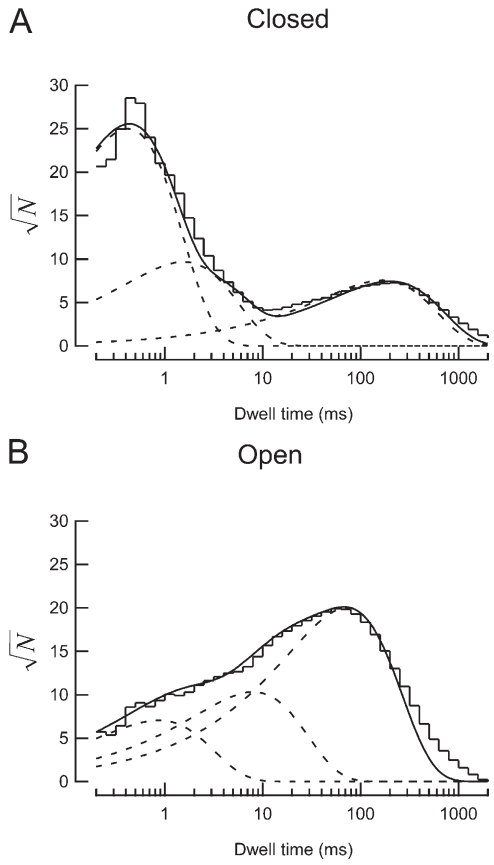

Figure 2. Example dwell-time histograms of single channel recordings. (A) Dwell-time histogram of the closed states of a single MEC-4d/10d + MEC-2 + MEC-6 channel. (B) Dwell-time histogram of the open states of the same channel as in A. For optimal visual estimation of fit quality (Sigworth and Sine, 1987), dwell times are accumulated into logarithmic bins and displayed with a square-root ordinate. Solid lines are fits to the data with the sum of three exponential functions, dotted lines represent each exponential component.

ions and measured the extent of current inhibition. In macropatches excised from oocytes coexpressing MEC-4d/10d + MEC-2 + MEC-6, both Ca^{2+} and Mg^{2+} inhibit current with millimolar affinity (Fig. 3). Like blockade by amiloride (Chelur et al., 2002; Goodman et al., 2002a), block by divalent ions is voltage dependent (Fig. 3), a result that suggests that divalent ions act as open-channel blockers. Divalent ions and amiloride bind to different sites, however, since inhibition by amiloride was unaffected by the presence of 1 mM Ca^{2+} and 2 mM Mg^{2+} (Fig. S1, available at http://www.jgp.org/cgi/content/full/jgp.200709910/DC1).

We also examined whether MEC-2 or MEC-6 alter block by Ca^{2+}. Both MEC-2 and MEC-6 decrease the apparent affinity for Ca^{2+} ions (Fig. 3). If Ca^{2+} is a permeant blocker, then increasing external [Ca^{2+}] should shift the reversal potential to more positive potentials. Consistent with this idea and with prior work demonstrating that MEC-4 channels are Ca^{2+} permeable (Bianchi et al., 2004), currents recorded in 10 mM Ca^{2+} reversed +1.8 ± 0.2 mV (n = 5) more positive than those recorded in nominally 0 mM Ca^{2+}. This small shift is consistent with ΔE_{rev} estimated using the Goldman-Hodgkin-Katz current (see Lewis, 1984), assuming the measured Ca^{2+} permeability P_{Ca}/P_{Na} = 0.22 (Bianchi et al., 2004). Channels containing only MEC-4d/10d were not analyzed since patches contained too few channels for analysis.

Protease Activates MEC-4-dependent Channels Independently of MEC-2 and MEC-6

Both native and expressed ENaCs can be activated by proteases (Planes and Caughey, 2007). It is not known whether proteases can also activate MEC-4/10 channels. We investigated this by applying chymotrypsin, a serine protease known to activate ENaCs (Chraibi et al., 1998), to MEC-4d/10d channels expressed in oocytes. As shown in Fig. 4, chymotrypsin application increases amiloride-sensitive currents in whole oocytes. The slight shift of reversal potential toward zero is likely due to sodium loading of the cell, and is observed on similar timescales when no protease is applied (unpublished data). Chymotrypsin increased current by approximately twofold in the presence and absence of MEC-2 and MEC-6, indicating that neither auxiliary protein affects sensitivity to proteases. These data indicate that the mechanisms by which protease and MEC-2/MEC-6 increase current are distinct.

MEC-2 and MEC-6 Promote Channel Activity without Increasing Surface Expression

By contrast with their dramatic effects on whole-cell current (Chelur et al., 2002; Goodman et al., 2002a), MEC-2 and MEC-6 have only modest effects on single-channel currents (Table I, Fig. 1, Table II, and Table III). We considered two possible explanations. First, auxiliary proteins could increase the total number of channels at

TABLE III

Open-State Dwell Times of Single MEC-4d/10d Channels and Effects of Auxiliary Subunits

	$<\tau_o>$(ms)	P_{o1}	τ_{o1} (ms)	P_{o2}	τ_{o2} (ms)	P_{o3}	τ_{o3} (ms)
MEC-4d/10d	250 ± 60 (11)	0.26 (3)	2.2 (3)	0.40 (3)	37 (3)	0.33 (3)	180 (3)
+MEC-2	340 ± 210 (7)	0.29 (3)	1.7 (3)	0.29 (3)	13 (3)	0.43 (3)	110 (3)
+MEC-6	490 ± 140 (4)	0.29 (2)	7.9 (2)	0.40 (2)	79 (2)	0.31 (2)	1200 (2)
+MEC-2 +MEC-6	240 ± 84 (5)	0.38 (4)	1.8 (4)	0.17 (3)	14 (4)	0.45 (4)	300 (4)

Average open-time, $<\tau_o>$ ANOVA: $F(3,22) = 0.58$, P = 0.64.

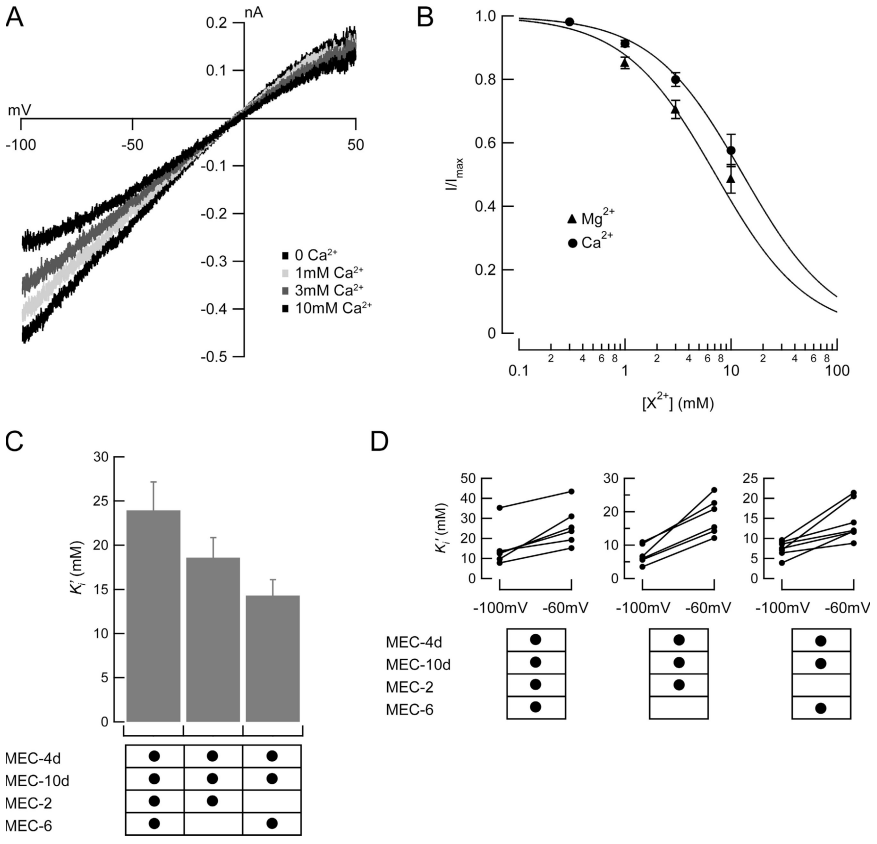

Figure 3. Block by divalent cations. (A) Macroscopic *I-V* curve of an outside-out patch coexpressing MEC-4d/10d, MEC-2, and MEC-6 exposed to varying Ca^{2+} concentrations. (B) Dose–response curves for blockade by Ca^{2+} and Mg^{2+} at −100 mV. The smooth curve is fit to the average values assuming a Hill coefficient of 1: $I = I_{max}(1 + [X^{2+}]/K_i')^{-1}$. Measured K_i' was 12.9 mM for Ca^{2+}, 7.0 mM for Mg^{2+}. (C) Apparent Ca^{2+} inhibition constant, K_i' as a function of auxiliary subunits. $V_{hold} = -60$ mV. (D) Voltage dependence and variation of block affinity. Each line represents a single patch, with K_i' measured at −60 and −100 mV.

the oocyte membrane. Prior work showing that neither MEC-2 (Goodman et al., 2002a) nor MEC-6 (Chelur et al., 2002) increases surface expression makes this explanation unlikely, however. Nonetheless, it is formally possible that surface expression increases when both MEC-2 and MEC-6 are present. We tested this idea by comparing the amount of myc-tagged MEC-4d expressed in the plasma membrane in the presence and absence of both MEC-2 and MEC-6. We found that addition of MEC-2 and MEC-6 did not produce a detectable change in the amount of myc-tagged MEC-4d protein in the plasma membrane (Fig. S2).

Second, the auxiliary proteins could act by increasing the fraction of active membrane-inserted channels. That is, in the absence of these subunits, active channels are rare, but exhibit properties similar to those bound to MEC-2 and MEC-6. To demonstrate this directly, we injected varying amounts of cRNA encoding MEC-2 along with constant amounts of cRNA encoding MEC-4d/10d and MEC-6. We measured current and surface protein levels in parallel and found that while surface protein level does not change detectably, current increases with the amount of MEC-2 cRNA (Fig. 5). Since MEC-2 cannot form channels by itself (Goodman et al., 2002a), has a modest effect on single-channel conductance, and has no effect on steady-state open probability, this finding demonstrates that increasing the amount of MEC-2 enhances current by increasing the fraction of membrane-inserted MEC-4d protein that carries current.

MEC-2 Palmitoylation and Cholesterol-binding Activity Are Required for Channel Activation

We also interrogated the mechanism by which MEC-2 activates channels. Specifically, we tested which aspects of MEC-2 function were required for its current-enhancing effect. As shown in Fig. 6, we targeted three residues involved in cholesterol binding: P134, C140, and C174. Replacing the wild-type cysteine with alanine at amino acids 140 and 174 eliminates palmitoylation and reduces cholesterol binding (Huber et al., 2006). Replacing the proline at 134 with serine recapitulates the *mec-2(u274)* allele, which causes touch insensitivity in vivo (Zhang et al., 2004a) and abolishes cholesterol binding in vitro (Huber et al., 2006). We found that coinjection of the palmitoylation mutant MEC-2(C140/174A) produces currents larger than those in the absence of MEC-2, but smaller than those recorded with wild-type MEC-2. Coinjection of MEC-2(P134S) produces none of the current enhancement provided by wild-type MEC-2 (Fig. 6); amiloride-sensitive currents were indistinguishable from those recorded in the absence of MEC-2. Currents produced by the triple mutant MEC-2(P134S, C140/174A) were indistinguishable from those produced by single mutant MEC-2(P134S) (Fig. 6).

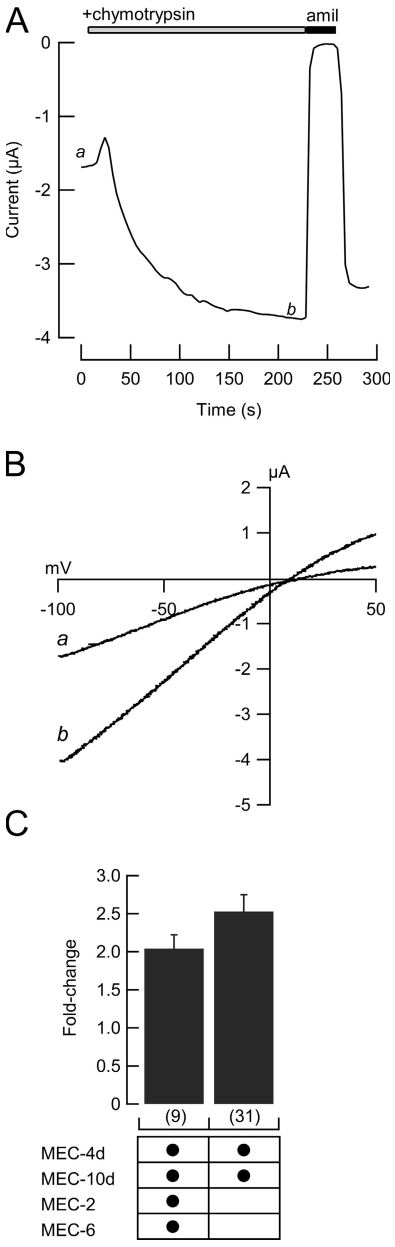

Figure 4. Activation by extracellular chymotrypsin. (A) Example time course of chymotrypsin-evoked current increase in an oocyte expressing MEC-4d/10d + MEC-2 + MEC-6. *a* and *b* indicate when the curves shown in B were collected. Current amplitude was measured every 4 s at −85 mV. (B) Whole-cell *I-V* relationship before (*a*) and during chymotrypsin application (*b*). In all cases, chymotypsin-evoked current was blocked by amiloride (300 μM). (C) Chymotrypsin-evoked increase in the amiloride-sensitive current in the presence and absence of MEC-2 and MEC-6.

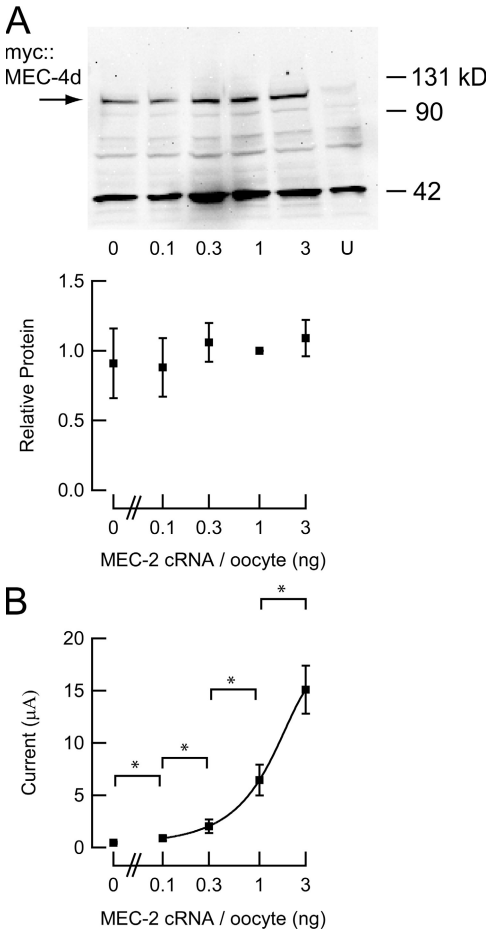

Figure 5. Surface expression and current amplitude as a function of MEC-2 cRNA. (A) Surface expression of myc::MEC-4d in oocytes coexpressing myc::MEC-4d, MEC-10d, MEC-2, and MEC-6 (top). The amount of MEC-2 cRNA is indicated below each lane; *U* indicates uninjected (control) oocytes. Relative surface expression as a function MEC-2 cRNA (bottom), normalized to density with 1 ng MEC-2 cRNA per oocyte. Data represent the results of three independent Western blots. Nonspecific bands are observed in all blots and are visible in uninjected cells. (B) Amiloride-sensitive currents recorded from oocytes analyzed in parallel with those used for Western blotting in A. Stars indicate significance $P < 0.01$ (Student's *t* test). Smooth line is fit to the data according to: $I = I_0 + (I_{max} - I_0)(1 + [\text{MEC-2 cRNA}]/EC_{50})^{-1}$. The EC_{50} is 2.8 ng, $I_O = 0.48$ μA.

Since MEC-2 increases single-channel conductance, γ, we also examined if the mutant form of MEC-2 retained the ability to increase γ. In six patches excised from oocytes expressing MEC-4d/10d + MEC-2(P134S, C140/174A) + MEC-6, the single channel conductance was similar to that of channels lacking MEC-2, and significantly different from channels with wild-type MEC-2 ($P < 0.01$). These data emphasize the importance of cholesterol binding for the modification of channel biophysics by MEC-2.

The inability of MEC-2 isoforms containing the P134S mutation to enhance macroscopic current cannot be explained by a lack of protein, since mutant MEC-2 isoforms were readily detected in whole-cell lysates. (Fig. 6). As shown previously (Huber et al., 2006), wild-type MEC-2 appeared as a doublet near the predicted molecular weight. The P134S mutation altered the relative intensity of the two bands. Though the molecular basis for this observation is unclear, one appealing possibility is that cholesterol-modified MEC-2 is the dominant

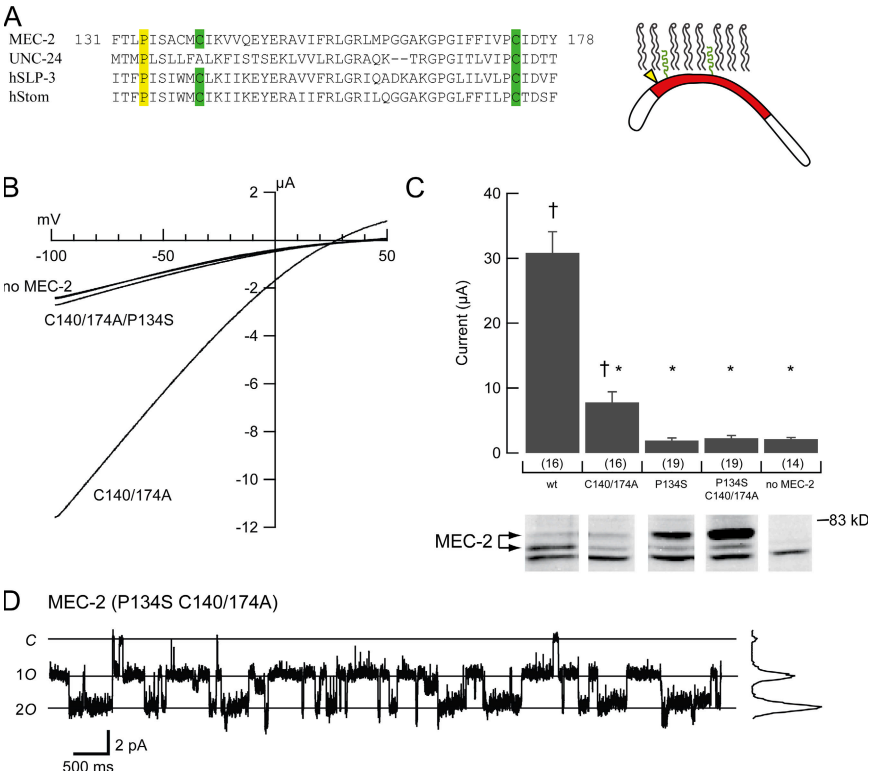

Figure 6. Characterization of cholesterol-binding mutants of MEC-2. (A) Alignment of selected PHB family members. MEC-2 and UNC-24 are coexpressed in vivo. MEC-2 is also represented schematically on the right. In yellow, P134, required for cholesterol binding. In green, C140 and C174 required for palmitoylation (Huber et al., 2006). (B) *I-V* relationship of channels lacking MEC-2, containing MEC-2 double mutant, and MEC-2 triple mutant. MEC-2(P134S) single mutant currents are essentially indistinguishable from the triple mutant and are omitted for clarity. (C) Average currents recorded from MEC-2 mutant-expressing cells (top). Bars are mean ± SEM. Sample size is indicated in parentheses below each bar. †, $P < 0.005$, compared with the absence of MEC-2; *, $P < 10^{-6}$ compared with wild-type MEC-2. Western blot of MEC-2 isoforms (bottom). For clarity, lanes corresponding to each isoform are aligned with the data in A. All lanes were from the same blot (with identical contrast manipulation). Similar results were obtained in a total of three independent experiments. (D) Single-channel activity from an outside-out patch of a cell expressing triple mutant MEC-2. These data were used to measure single-channel conductance. Solid lines indicate zero, one or both channels open; all-points histogram is shown on the right.

isoform and, like cholesterol-bound Hedgehog protein (Porter et al., 1996), migrates more quickly than the isoform lacking cholesterol.

These findings suggest that cholesterol binding enhances channel activity and imply that depleting membrane cholesterol should decrease current. To test this, we treated oocytes expressing MEC-4d+ MEC-2 with a cholesterol synthesis inhibitor (pravastatin) and a cholesterol chelator (methyl-β-cyclodextrin). This dual treatment was designed to mitigate differences in membrane cholesterol between animals as well to deplete membrane cholesterol. In cells harvested from one animal (out of six), this treatment significantly decreased ($P < 0.005$) amiloride-sensitive current compared with untreated control cells harvested from the same animal: 24.6 ± 2.5 μA ($n = 17$) vs. 41.3 ± 4.7 μA ($n = 14$). These results, while suggestive, are inconclusive and suggest that sensitivity to this treatment depends on an unknown factor that varies between animals.

DISCUSSION

What Defines an Active MEC-4 Channel Complex?

Here we present data showing that MEC-2 and MEC-6 govern transitions between an unavailable or silent state and one in which MEC-4d/10d channels are available to be activated. Based on these data, we propose that the MEC-2 and MEC-6 auxiliary subunits are permissive regulators of MEC-4 sensory mechanotransduction channels both in heterologous cells and in vivo. Consistent with this model, MEC-2 is required for force-dependent gating in vivo (O'Hagan et al., 2005). The in vivo role of MEC-6 is more complex, since it is also required for channel localization (Chelur et al., 2002).

This study also demonstrates the existence of multiple closed and open states in constitutively active channels. How these states might be involved in the regulation and activity of the channel is not yet clear, but the analysis does reveal a complexity of gating. Except for a MEC-2–dependent 30% increase in γ, MEC-4d/10d channel behavior is qualitatively and quantitatively similar in the absence or presence of MEC-2, MEC-6, or both MEC-2 and MEC-6.

Divalents and the MEC-4 Sensory Transduction Channel

We have shown that the divalent ions Ca^{2+} and Mg^{2+} block channels formed by the MEC-4 complex in a voltage-dependent manner. A voltage-dependent block of similar affinity has been reported in certain mutant versions of ENaC (Schild et al., 1997) and in the related acid-sensing ion channels (ASICs) (Waldmann et al., 1997; de Weille and Bassilana, 2001).

One interesting consequence of block by divalent ions is that a significant fraction of current in whole-cell

recordings has likely been blocked by divalents in control recording solutions. Also, due to the difference in divalent affinity between channels with and without MEC-2 and MEC-6 (Fig. 3), a larger fraction of current would be blocked in cells lacking MEC-2 and MEC-6. This would have led to an underestimate of current in these cells and accounts for some fraction of the increase in macroscopic current ascribed to MEC-2 and MEC-6. If this difference in affinity for block by divalent ions was the only effect of MEC-2 and MEC-6, coexpression of the auxiliary subunits would increase current by 50%. As this maneuver increases current by ~100-fold (Chelur et al., 2002), a difference in divalent block only accounts for a small fraction of the effect of auxiliary subunits.

The Role of MEC-10 in the Complex

Several lines of evidence point to MEC-10 as an inhibitory unit of the sensory transduction channel. First, MEC-10–induced neurodegeneration is a weaker phenotype that can be suppressed by many alleles of other *mec* genes (Huang and Chalfie, 1994). Second, while MEC-10 is not required for MEC-4 channel activity in oocytes, coexpressing MEC-10 decreases macroscopic current (Goodman et al., 2002a). However, the effect of MEC-10 on single-channel properties seems to be small or nonexistent. Comparing our present results for channels composed of MEC-4d/10d and MEC-2 to values previously reported for channels composed only of MEC-4d and MEC-2, we find γ_2 (38.3 pS vs. 38.0 pS) and P_o (0.79 vs. 0.86) to be very similar. Taken together, these results indicate that MEC-10 may regulate the MEC-4 channel complex activity by a similar mechanism to that proposed for MEC-2 and MEC-6, that is, by controlling the number of channels accessible for activation. However, the synergistic current enhancement given by MEC-2 and MEC-6 is largely independent of the presence of MEC-10 (Goodman et al., 2002a; Chelur et al., 2002), suggesting that these effects work in parallel.

The Interaction between MEC-2 and the Channel Pore

MEC-2, which cannot form channels on its own and is associated only with the inner leaflet of the plasma membrane, modifies the MEC-4 channel pore. Two lines of evidence support this conclusion. First, MEC-2 decreases the affinity of the MEC-4 channel for two open channel blockers: amiloride (Chelur et al., 2002) and divalent ions (this study). Second, MEC-2 significantly increases single-channel conductance. These effects could reflect a long-range conformational change in the channel pore produced by MEC-2, cholesterol binding, or both. Alternatively, they could indicate that MEC-2 directly modifies the inner vestibule of the channel. Additional studies will be required to distinguish among these possibilities. One region of MEC-2 that could affect the inner vestibule and account for the ability of MEC-2 to increase single channel conductance is a stretch of negatively charged amino acids (297–314) that could potentially concentrate Na^+ ions near the pore. In support of this idea, three glutamate residues (E297, E299, and E314) are mutated to lysine in three *mec-2* alleles (*u318*, *e1514*, and *u217*, respectively) that disrupt touch insensitivity in vivo (Zhang et al., 2004a).

Could Accessory Proteins Regulate Membrane Environment?

Membrane environment is intimately tied to channel function, with particular regard to proteins that sense force (Anishkin and Kung, 2005). This is most obvious in channels that can be activated by membrane stretch alone, such as MscL and MscS, but could be equally important in the activation of channels by force delivered through other modalities. Several recent models propose methods to couple membrane properties such as curvature, thickness, and fluidity to force activation (Markin and Sachs, 2004; Moe and Blount, 2005). The cocrystallization of head groups of detergent molecules in the recent ASIC1 structure (Jasti et al., 2007) provides evidence that hydrophobic molecules, including lipids, may also bind channels directly.

An appealing possibility is raised by the cholesterol and fatty acid binding properties of MEC-2 and the importance of these properties for function. MEC-2 can easily be conceived as having a strong role in regulating the membrane environment of the channel, either by localizing the complex to regions of high cholesterol or by directly recruiting cholesterol to the area of the membrane surrounding the channel. This hypothesis is supported by the observation that MEC-2 oligomerizes (Zhang et al., 2004a; Huber et al., 2006) and our finding that MEC-2 enhances channel activity in a dose-dependent manner. MEC-2 may alter membrane environment as a function of the quantity of protein present by increasing cholesterol concentration proportionately. This could be a consequence of cholesterol's putative role in local thickening and stiffening of the bilayer and shifting the lateral pressure profile (Cantor, 1999; Gandhavadi et al., 2002; Niemela et al., 2007).

The membrane environment is potentially a unifying mechanism for the roles of MEC-2 and MEC-6. While nothing is known about the affinity of MEC-6 for cholesterol or other membrane components, paraoxonases are known to be associated with HDL particles (Draganov et al., 2000) and PON1 has one nontransmembrane helix proposed to mediate lipid interaction via aromatic amino acids (Harel et al., 2004). This helix is likely present in MEC-6, and several of the highlighted aromatic amino acids are conserved; we propose that this helix may enhance lipid association in MEC-6 as well. While it remains highly speculative, the modes of action and

synergism of MEC-2 and MEC-6 could be explained if each regulates the membrane environment on its respective leaflet of the bilayer, MEC-2 on the intracellular and MEC-6 on the extracellular side. Thus, the membrane environment is likely to be a critical parameter of channel activity and, possibly, of force-dependent gating in vivo.

We thank G. Martinez and B. Johnson for suggestions regarding the manuscript.

This work was supported by National Institutes of Neurological Disorders and Stroke (NS047715), the American Heart Association, Western States Affiliate, the A. P. Sloan and Donald B. and Delia E. Baxter Foundations, the Klingenstein Fund and McKnight Endowment, and an American Heart Association predoctoral fellowship (Western States Affiliate) to A.L. Brown.

Olaf S. Andersen served as editor.

Submitted: 18 October 2007
Accepted: 5 May 2008

REFERENCES

Anishkin, A., and C. Kung. 2005. Microbial mechanosensation. *Curr. Opin. Neurobiol.* 15:397–405.

Bengrine, A., J. Li, L.L. Hamm, and M.S. Awayda. 2007. Indirect activation of the epithelial Na^+ channel by trypsin. *J. Biol. Chem.* 282:26884–26896.

Bianchi, L., B. Gerstbrein, C. Frokjaer-Jensen, D.C. Royal, G. Mukherjee, M.A. Royal, J. Xue, W.R. Schafer, and M. Driscoll. 2004. The neurotoxic MEC-4(d) DEG/ENaC sodium channel conducts calcium: implications for necrosis initiation. *Nat. Neurosci.* 7:1337–1344.

Brown, A.L., S.M. Fernandez-Illescas, Z. Liao, and M.B. Goodman. 2007. Gain-of-function mutations in the MEC-4 DEG/ENaC sensory mechanotransduction channel alter gating and drug blockade. *J. Gen. Physiol.* 129:161–173.

Caldwell, R.A., R.C. Boucher, and M.J. Stutts. 2004. Serine protease activation of near-silent epithelial Na^+ channels. *Am. J. Physiol. Cell Physiol.* 286:C190–C194.

Cantor, R.S. 1999. Lipid composition and the lateral pressure profile in bilayers. *Biophys. J.* 76:2625–2639.

Chalfie, M., and E. Wolinsky. 1990. The identification and suppression of inherited neurodegeneration in *Caenorhabditis elegans*. *Nature.* 345:410–416.

Chelur, D.S., G.G. Ernstrom, M.B. Goodman, C.A. Yao, L. Chen, R. O'Hagan, and M. Chalfie. 2002. The mechanosensory protein MEC-6 is a subunit of the *C. elegans* touch-cell degenerin channel. *Nature.* 420:669–673.

Chillaron, J., R. Estevez, I. Samarzija, S. Waldegger, X. Testar, F. Lang, A. Zorzano, A. Busch, and M. Palacin. 1997. An intracellular trafficking defect in type I cystinuria rBAT mutants M467T and M467K. *J. Biol. Chem.* 272:9543–9549.

Chraibi, A., V. Vallet, D. Firsov, S.K. Hess, and J.D. Horisberger. 1998. Protease modulation of the activity of the epithelial sodium channel expressed in *Xenopus* oocytes. *J. Gen. Physiol.* 111:127–138.

de Weille, J., and F. Bassilana. 2001. Dependence of the acid-sensitive ion channel, ASIC1a, on extracellular Ca^{2+} ions. *Brain Res.* 900:277–281.

Draganov, D.I., P.L. Stetson, C.E. Watson, S.S. Billecke, and B.N. La Du. 2000. Rabbit serum paraoxonase 3 (PON3) is a high density lipoprotein-associated lactonase and protects low density lipoprotein against oxidation. *J. Biol. Chem.* 275:33435–33442.

Driscoll, M., and M. Chalfie. 1991. The *mec-4* gene is a member of a family of *Caenorhabditis elegans* genes that can mutate to induce neuronal degeneration. *Nature.* 349:588–593.

Gandhavadi, M., D. Allende, A. Vidal, S.A. Simon, and T.J. McIntosh. 2002. Structure, composition, and peptide binding properties of detergent soluble bilayers and detergent resistant rafts. *Biophys. J.* 82:1469–1482.

Goodman, M.B., and S.R. Lockery. 2000. Pressure polishing: a method for re-shaping patch pipettes during fire polishing. *J. Neurosci. Methods.* 100:13–15.

Goodman, M.B., G.G. Ernstrom, D.S. Chelur, R. O'Hagan, C.A. Yao, and M. Chalfie. 2002a. MEC-2 regulates *C. elegans* DEG/ENaC channels needed for mechanosensation. *Nature.* 415:1039–1042.

Goodman, M.B., G.G. Ernstrom, D.S. Chelur, R. O'Hagan, C.A. Yao, and M. Chalfie. 2002b. Corrigendum: MEC-2 regulates *C. elegans* DEG/ENaC channels needed for mechanosensation. *Nature.* 417:880.

Harel, M., A. Aharoni, L. Gaidukov, B. Brumshtein, O. Khersonsky, R. Meged, H. Dvir, R.B. Ravelli, A. McCarthy, L. Toker, et al. 2004. Structure and evolution of the serum paraoxonase family of detoxifying and anti-atherosclerotic enzymes. *Nat. Struct. Mol. Biol.* 11:412–419.

Huang, M., and M. Chalfie. 1994. Gene interactions affecting mechanosensory transduction in *Caenorhabditis elegans*. *Nature.* 367:467–470.

Huang, M., G. Gu, E.L. Ferguson, and M. Chalfie. 1995. A stomatin-like protein necessary for mechanosensation in *C. elegans*. *Nature.* 378:292–295.

Huber, T.B., B. Schermer, R.U. Muller, M. Hohne, M. Bartram, A. Calixto, H. Hagmann, C. Reinhardt, F. Koos, K. Kunzelmann, et al. 2006. Inaugural article: podocin and MEC-2 bind cholesterol to regulate the activity of associated ion channels. *Proc. Natl. Acad. Sci. USA.* 103:17079–17086.

Hughey, R.P., J.B. Bruns, C.L. Kinlough, K.L. Harkleroad, Q. Tong, M.D. Carattino, J.P. Johnson, J.D. Stockand and T.R. Kleyman. 2004. Epithelial sodium channels are activated by furin-dependent proteolysis. *J. Biol. Chem.* 279:18111–18114.

Jasti, J., H. Furukawa, E.B. Gonzales, and E. Gouaux. 2007. Structure of acid-sensing ion channel 1 at 1.9 Å resolution and low pH. *Nature.* 449:316–323.

Johansson, R.S., and A.B. Vallbo. 1979. Detection of tactile stimuli. Thresholds of afferent units related to psychophysical thresholds in the human hand. *J. Physiol.* 297:405–422.

Kellenberger, S., and L. Schild. 2002. Epithelial sodium channel/degenerin family of ion channels: a variety of functions for a shared structure. *Physiol. Rev.* 82:735–767.

Lai, C.C., K. Hong, M. Kinnell, M. Chalfie, and M. Driscoll. 1996. Sequence and transmembrane topology of MEC-4, an ion channel subunit required for mechanotransduction in *Caenorhabditis elegans*. *J. Cell Biol.* 133:1071–1081.

Levina, N., S. Totemeyer, N.R. Stokes, P. Louis, M.A. Jones, and I.R. Booth. 1999. Protection of *Escherichia coli* cells against extreme turgor by activation of MscS and MscL mechanosensitive channels: identification of genes required for MscS activity. *EMBO J.* 18:1730–1737.

Lewis, C.A. 1984. Divalent cation effects on acetylcholine-activated channels at the frog neuromuscular junction. *Cell. Mol. Neurobiol.* 4:273–284.

Mannsfeldt, A.G., P. Carroll, C.L. Stucky, and G.R. Lewin. 1999. Stomatin, a MEC-2 like protein, is expressed by mammalian sensory neurons. *Mol. Cell. Neurosci.* 13:391–404.

Markin, V.S., and F. Sachs. 2004. Thermodynamics of mechanosensitivity. *Phys. Biol.* 1:110–124.

Martinez-Salgado, C., A.G. Benckendorff, L.Y. Chiang, R. Wang, N. Milenkovic, C. Wetzel, J. Hu, C.L. Stucky, M.G. Parra, N.

Mohandas, and G.R. Lewin. 2007. Stomatin and sensory neuron mechanotransduction. *J. Neurophysiol.* 98:3802–3808.

Moe, P., and P. Blount. 2005. Assessment of potential stimuli for mechano-dependent gating of MscL: effects of pressure, tension, and lipid headgroups. *Biochemistry.* 44:12239–12244.

Niemela, P.S., S. Ollila, M.T. Hyvonen, M. Karttunen, and I. Vattulainen. 2007. Assessing the nature of lipid raft membranes. *PLoS Comput. Biol.* 3:e34.

O'Hagan, R., M. Chalfie, and M.B. Goodman. 2005. The MEC-4 DEG/ENaC channel of *Caenorhabditis elegans* touch receptor neurons transduces mechanical signals. *Nat. Neurosci.* 8:43–50.

Planes, C., and G.H. Caughey. 2007. Regulation of the epithelial Na^+ channel by peptidases. *Curr. Top. Dev. Biol.* 78:23–46.

Porter, J.A., K.E. Young, and P.A. Beachy. 1996. Cholesterol modification of hedgehog signaling proteins in animal development. *Science.* 274:255–259.

Schild, L., E. Schneeberger, I. Gautschi, and D. Firsov. 1997. Identification of amino acid residues in the α, β, and γ subunits of the epithelial sodium channel (ENaC) involved in amiloride block and ion permeation. *J. Gen. Physiol.* 109:15–26.

Sedensky, M.M., J.M. Siefker, J.Y. Koh, D.M. Miller III, and P.G. Morgan. 2004. A stomatin and a degenerin interact in lipid rafts of the nervous system of *Caenorhabditis elegans*. *Am. J. Physiol. Cell Physiol.* 287:C468–C474.

Sigworth, F.J., and S.M. Sine. 1987. Data transformations for improved display and fitting of single-channel dwell time histograms. *Biophys. J.* 52:1047–1054.

Vallet, V., C. Pfister, J. Loffing, and B.C. Rossier. 2002. Cell-surface expression of the channel activating protease xCAP-1 is required for activation of ENaC in the *Xenopus* oocyte. *J. Am. Soc. Nephrol.* 13:588–594.

Waldmann, R., G. Champigny, F. Bassilana, C. Heurteaux, and M. Lazdunski. 1997. A proton-gated cation channel involved in acid-sensing. *Nature.* 386:173–177.

Wetzel, C., J. Hu, D. Riethmacher, A. Benckendorff, L. Harder, A. Eilers, R. Moshourab, A. Kozlenkov, D. Labuz, O. Caspani, et al. 2007. A stomatin-domain protein essential for touch sensation in the mouse. *Nature.* 445:206–209.

Yeung, D.T., D.E. Lenz, and D.M. Cerasoli. 2005. Analysis of active-site amino-acid residues of human serum paraoxonase using competitive substrates. *FEBS J.* 272:2225–2230.

Zhang, S., J. Arnadottir, C. Keller, G.A. Caldwell, C.A. Yao, and M. Chalfie. 2004a. MEC-2 is recruited to the putative mechanosensory complex in *C. elegans* touch receptor neurons through its stomatin-like domain. *Curr. Biol.* 14:1888–1896.

Zhang, S., C. Ma, and M. Chalfie. 2004b. Combinatorial marking of cells and organelles with reconstituted fluorescent proteins. *Cell.* 119:137–144.